Journal of Polymer Science and Engineering (2023) Volume 6 Issue 1
doi: 10.24294/jpse.v6i1.3208

ORIGINAL RESEARCH ARTICLE

Cadmium selenium quantum dot based nanosensor with femto molar level sensitivity for the detection of the pesticide endosulfan

Lakshmi V Nair[1,2], Resmi V Nair[1,3], Ramapurath S Jayasree[1,*]

[1] *Division of Biophotonics and Imaging, Biomedical Technology Wing, Sree Chitra Tirunal Institute for Medical Sciences and Technology, Kerala 695011, India*

[2] *School of Mechanical and Materials Engineering, The University of Alabama at Birmingham, Birmingham, AL 35233, USA*

[3] *Programmable Molecular Design Lab, Jawaharlal Nehru Centre for Advanced Scientific Research, Bangalore 560064, India*

*** Corresponding author:** Ramapurath S Jayasree, jayasree@sctimst.ac.in

ABSTRACT

Endosulfan (6,7,8,9,10,10-Hexachloro-1,5,5a,6,9,9a-hexahydro-6,9-methano-2,4,3-benzodioxathiepine-3-oxide) is an off-patent insecticide used in agricultural farms. Its usage as a pesticide has become highly controversial over the last few decades. This is due to its reported hazardous nature to health and side effects like growth retardation, hydrocephalus, and undesired changes in the male and female hormones leading to complications in sexual maturity. Endosulfan is the main culprit among all pesticide poisoning incidents around the world. Though the usage of this dreaded pesticide is banned by most countries, the high stability of this molecule to withstand degradation for a long period poses a threat to mankind even today. So, it has become highly essential to detect the presence of this poisonous pesticide in the drinking water and milk around these places. It is also advisable to check the presence of this toxic material in the blood of the population living in and around these places so that an early and appropriate management strategy can be adopted. With this aim, we have developed a sensor for endosulfan that displayed high selectivity and sensitivity among all other common analytes in water and biological samples, with a wide linear concentration range (2 fM to 2 mM), a low detection limit (2 fM), and rapid response. A citrate-functionalized cadmium-selenium quantum dot was used for this purpose, which showed a concentration-dependent fluorescence enhancement, enabling easy and sensitive sensing. This sensor was utilized to detect endosulfan in different sources of water, human blood serum, and milk samples with good recoveries. It is also noted that the quantum dot forms a stable complex with endosulfan and is easy to separate from the contaminated source, paving the way for purifying the contaminated water. More detailed tests and validation of the sensor are needed to confirm these observations.

Keywords: endosulfan; quantum dot; sensor; femtomolar sensitivity; water pollution; pesticide

ARTICLE INFO

Received: 8 November 2023
Accepted: 10 December 2023
Available online: 19 December 2023

1. Introduction

Pesticides are chemical substances used to destroy pests that attack crops in the agricultural field. Endosulfan is an off-patent organochlorine insecticide. It belongs to a class of persistent organic pesticides (POP), which are a set of toxic chemicals that persist in the environment for years before breaking down into harmless molecules[1]. These chemicals circulate globally; those released in one part of the world can get deposited far away from their original source through a process of deposition and evaporation. Since it is sprayed onto the crops, the whole food chain gets affected by the repeated circulation of the pesticide.

Endosulfan exposure is linked to different medical conditions, such as physical deformities, neurotoxicity, poisoning, etc. A large number of neighboring populations have been victimized by the use of this pesticide, resulting in a broad range of diseases, from growth retardation to hydrocephalus, which has created horror in such areas[2]. It is reported that it can imitate or enhance the effect of female hormones[3]. Delayed sexual maturity in boys was reported in many places as an after-effect of the influence of this pesticide[4]. POPs are lipophilic, and hence they accumulate in fatty tissues. Concentrations of these chemicals in fatty tissues can be magnified to about 70,000 times higher than the background levels. It is a widely banned pesticide due to its hazardous effects on human endocrine and genetic systems. These pesticides accumulate in the environment and thereby affect food chains. Moreover, its presence in water can bioconcentrate in aquatic organisms.

It is known that endosulfan tends to persist in soil without degradation for a longer duration, transport over long distances, and accumulate in living organisms, creating harmful effects for them. Hence, the detection of the remaining residue and its removal play an important role in the near future. Even after the ban, the presence of residual pesticides in the soil and water sources in very low concentrations cannot be ruled out and hence demands the need for a very sensitive sensor. The commonly employed techniques for the detection of endosulfan include liquid chromatography mass spectrometry (LC-MS)[5], gas chromatography mass spectrometry (GC-MS)[6], high-performance liquid chromatography (HPLC)[7], gold immunochromatographic strips and indirect competitive ELISA[8], multiwalled carbon nanotube-based sensor[9] etc. Currently, available detection techniques are limited by several factors, including low sensitivity. It is reported that 0.21 to 54 ng/L of endosulfan is present in the drinking water near the endosulfan-sprayed farms[10].

Nanoparticles, being extremely small in size, have high reactivity and size-tuneable properties, which makes them suitable for many applications[11–25]. Quantum dots (Qd) have gained wide attention in this field due to their favorable optical properties and low cost[26–28]. Cadmium sulfide (cds) quantum dots were previously shown to be a sensor for endosulfan using the fluorescence immunoassay technique[29]. A spectrophotometric mode of detection of endosulfan using metal nanoparticles has been previously reported by Sreekumaran Nair et al.[30]. Electrochemical, enzymatic, and non-enzymatic-based endosulfan detection were demonstrated using different nanoparticles[31–33].

With this background, we aim to develop a highly selective and sensitive nanosensor using citrate-stabilized cadmium selenium quantum dots for the detection of endosulfan, augmented by the new science of nanotechnology. The sensor, with femtomolar level sensitivity, has the potential to detect endosulfan in different environments.

2. Materials and method

All the reagents were used as supplied without further purification unless stated. Cadmium acetate, trisodium citrate, selenium, and sodium sulphite of analytical grade were purchased from Merck India.

2.1. Instrumentation

UV-Visible (UV-Vis) absorbance spectra were recorded using a double beam spectrophotometer (Shimadzu, Japan) from 300 nm to 800 nm. A photoluminescence study was performed using a Cary Bio 500 instrument using a 1 cm path length cuvette. A Nicolet 5700 in Madison, USA, recorded the Fourier transform infrared spectroscopy—attenuated total reflectance (FTIR-ATR mode). JEOL 3010 at 300 KV was used to obtain high-resolution transmission electron microscope (HRTEM) micrographs of the material. For HRTEM analysis, samples were drop-cast into a formvar-coated copper grid. Samples were dried before the analysis. Dynamic light scattering (DLS) was performed with Nano ZS (Malvern, UK) for zeta potential measurement by dispersing the sample in water.

2.2. Synthesis of CdSe quantum dots

Cadmium selenium quantum dots were prepared using trisodium citrate as the stabilizing agent. Synthesis is done in a two-step process. Initially, sodium selino sulfite was synthesized. Briefly, 40 mM sodium sulphite solution was mixed with selenium metal powder and stirred at 75 °C till the solution became colourless. For the synthesis of quantum dots, 30 mM cadmium acetate was dissolved in 5 mL deionized (DI) water. 60 mM trisodium citrate was added to the cadmium solution in 15 mL dimethylformamide (DMF). When the solution became turbid, 55 mL water was added and stirred. To the above system 8×10^{-4} moles of freshly prepared selenium solution were added and stirred till the solution became colourless to reddish colour.

The prepared quantum dots were washed with isopropanol and centrifuged twice to purify the same.

2.3. Sensing of endosulfan in DI water, pipe water, well water and pond water

About 1mg of the developed quantum dots were dispersed in 1 mL of DI water to be used as the nanosensor. Different concentrations of endosulfan-containing water were added to the quantum dot solution.

2.4. Sensing of endosulfan in serum and milk

Human blood serum collected from the blood bank (Ethics committee approval number SCT/IEC/594/APRIL-2014) was separated and incubated with different concentrations of endosulfan. Concentration-dependent fluorescence was recorded upon the addition of endosulfan-incubated serum with Qd. Similarly, endosulfan in milk was also detected.

3. Results and discussion

3.1. Preparation of citrate capped cadmium selenium quantum dot

Quantum dots have gained wide attention in the fields of imaging, diagnosis, sensing, etc. due to their size-tuneable optical properties, low cost, high stability, and ease of synthesizing. Cadmium selenium quantum dots were synthesized by the pure wet chemical method. Stability of the QDs can be enhanced via surface functionalization or interaction with other molecules. Substances such as trioctyl phosphine (TOP) and tri-n-octylphosphine oxide (TOPO) are commonly used capping agents, which form water-insoluble QDs due to the hydrophobic nature of these organic solvents. Here, trisodium citrate is used as the capping agent.

The developed quantum dot has a characteristic broad absorption peak (**Figure 1a**) at 552 nm. The bulk CdSe particles have an absorbance maximum at 698 nm, which is absent in the prepared quantum dots, and the blue shift in the absorbance peak indicates a quantum confinement effect, confirming the formation of CdSe quantum dots[16,34,35]. The band gap of the CdSe quantum dot capped with trisodium citrate was estimated at 2.07 eV, which determines the unique properties of the developed nanomaterial. It has a maximum excitation at 448 nm with a shoulder band at 482 nm (**Figure A1**).

Excitation at 448 nm resulted in the maximum fluorescence emission at 570 nm (**Figure 1b**). Quantum confinement and interaction of the ligand with CdSe contribute to the green emission of the quantum dots. Qds showed a greenish-yellow emission under UV irradiation (**Figure 1b** inset). Transmission electron micrographs of CdSe quantum dots showed dispersed spherical particles (**Figure 2a**). The particle size distribution (**Figure 2b**) of the quantum dot showed an average size of 3.5 nm from the TEM micrographs (**Figure 2b**).

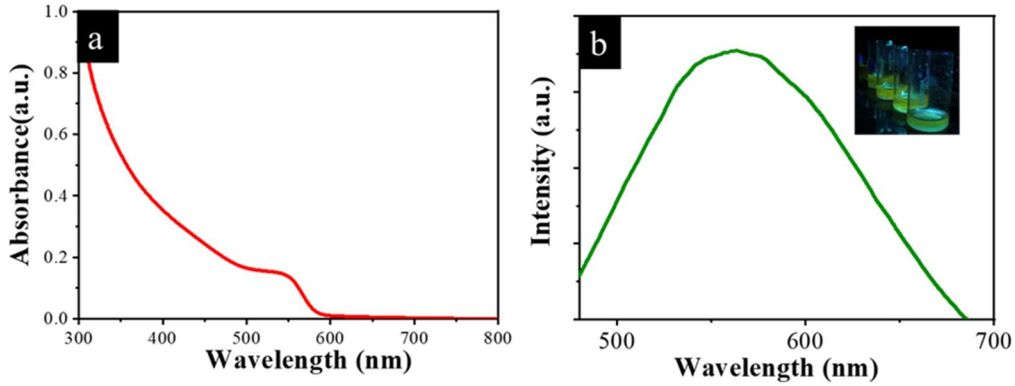

Figure 1. (a) UV-Vis absorption and **(b)** emission spectra of developed CdSe quantum dots. Inset of **(b)** shows the photograph of quantum dots under UV light irradiation.

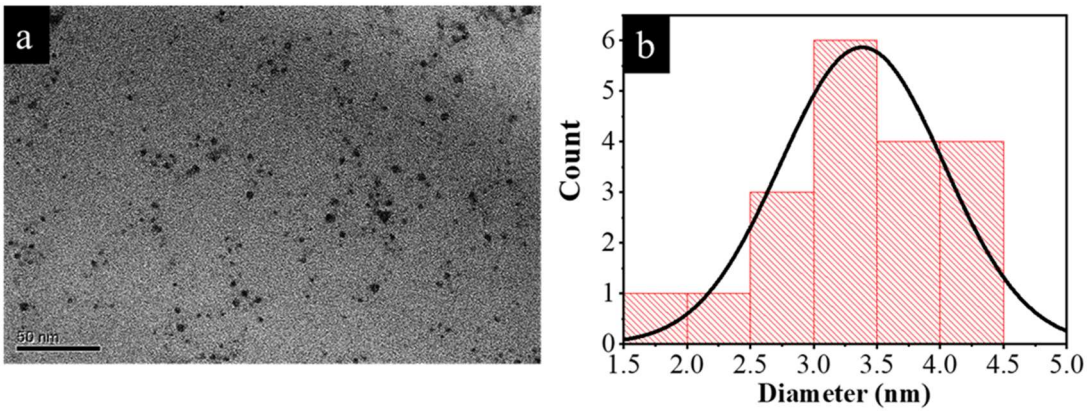

Figure 2. (a) Transmission electron micrographs of CdSe quantum; **(b)** corresponding particle size distribution of Qd.

3.2. Endosulfan detection

1 mg of citrate-capped quantum dots dissolved in 1 mL of DI water formed the nanosensor. Different concentrations of endosulfan (2 fM to 10 mM) were added to this colloidal nanosensor, i.e., citrate-stabilized quantum dots. The tested water was confirmed for the absence of endosulfan spectrometrically before the sensing efficacy was attempted.

To check the concentrations of endosulfan in real water sources (well water, pond water, and pipe water), the fluorescence spectrum was recorded after the addition of different concentrations of analyte. Sensing experiments were repeated three times in different media. As a sensing indicator, a concentration-dependent fluorescence enhancement of the 570 nm emission peak was observed with the addition of endosulfan to the Qd sensor (**Figures 3a, 3c**, and **A2**). In all the cases, fluorescence intensity increased with the concentration of endosulfan (**Figures 3a**, **3c**, and **A2**). The linear dependency of endosulfan detection was checked in the range from millimolar to femtomolar levels. DI water showed regression co-efficient value of 0.98 and well water showed 0.99 (**Figures 3b** and **3d**) indicating the high efficacy of developed sensor in the detection of endosulfan from these sources. In the cases of pipe water and pond water, the regression coefficient was slightly lower, which may be due to the presence of other molecules of water purifying agents and detergents, respectively, which we haven't included in the selectivity tests (**Figure A3**). The increase in fluorescence intensity is attributed to the binding of endosulfan to the quantum dot and subsequent enhancement in the light absorption by the quantum dot-endosulfan complex, as reflected in the absorption spectra of the complex with different concentrations of endosulfan (**Figure A4**). **Scheme 1** represents the binding of endosulfan to CdSe quantum dots.

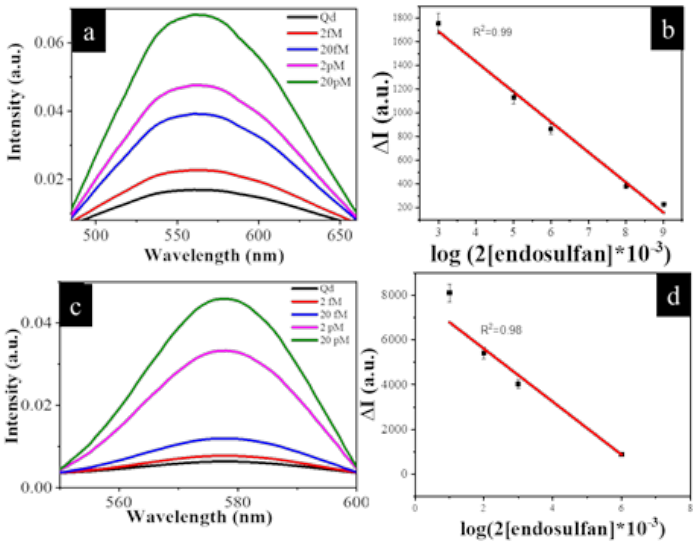

Figure 3. Endosulfan detection using the quantum dots in **(a)** DI water, **(b)** corresponding linear relation from millimolar to femtomolar range, **(c)** well water and **(d)** corresponding linear relation from millimolar to femtomolar range.

To understand more about the interaction of endosulfan with Qd and to explain the observed mechanism, detailed analysis of the complex was carried out using XRD, FT-IR, and zeta potential studies. A concentration-dependent increase in the surface charge was observed in the zeta potential (**Figure 4a**) of the sensor with different concentrations of endosulfan. This can be attributed to the presence of endosulfan, one of the most stable pesticides over Qd. Due to the presence of endosulfan over the quantum dot surface, the stability of the system increases, as is clear from the significant increase in the zeta potential with the increase in concentration.

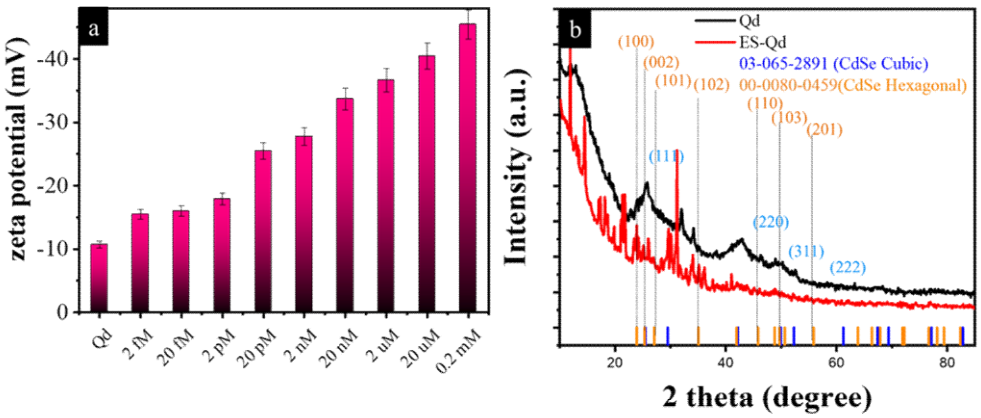

Figure 4. (a) Zeta potential evaluation of Qd and Qd with different concentrations of endosulfan (n = 3). **(b)** XRD pattern of Qd and endosulfan-treated Qd along with JCPDS data.

FT-IR spectroscopy and XRD evaluation further confirmed the binding of ES with Qd. The FT-IR spectrum (**Figure A5**) of the endosulfan-treated quantum dot showed all the characteristic peaks of both Qd and endosulfan with a slight shift, especially in the peaks of endosulfan. The characteristic -OH vibration was observed at 3353 cm^{-1} in CdSe Qd. The same peak was observed after ES complexation, indicating the presence of a hydroxyl group in the combined system. COO- peak at 1598 cm^{-1} was observed for both Qd sensors as well as for the combined system. The characteristic peaks of endosulfan seen at 1604 cm^{-1}, 1270 cm^{-1}, 1070 cm^{-1}, C = C, S = O, C-Cl got shifted to 1597 cm^{-1}, 1256 cm^{-1}, 1067 cm^{-1} after binding to the Qd. The shift in the vibrational modes to the lower wavenumber region indicates the formation of strong hydrogen bonds during the complex formation. In the case of S = O, a shift in wavelength of more than 10 cm^{-1} was

observed, which indicates that an electronic interaction followed by bond change occurred in ES on adding to Qd. From this observation, it can be confirmed that ES binds to Qd through S = O bond. The peaks corresponding to citrate were also present in the combined system, which indicates that the ES binding occurs through only one plane without disturbing the other planes of Qds.

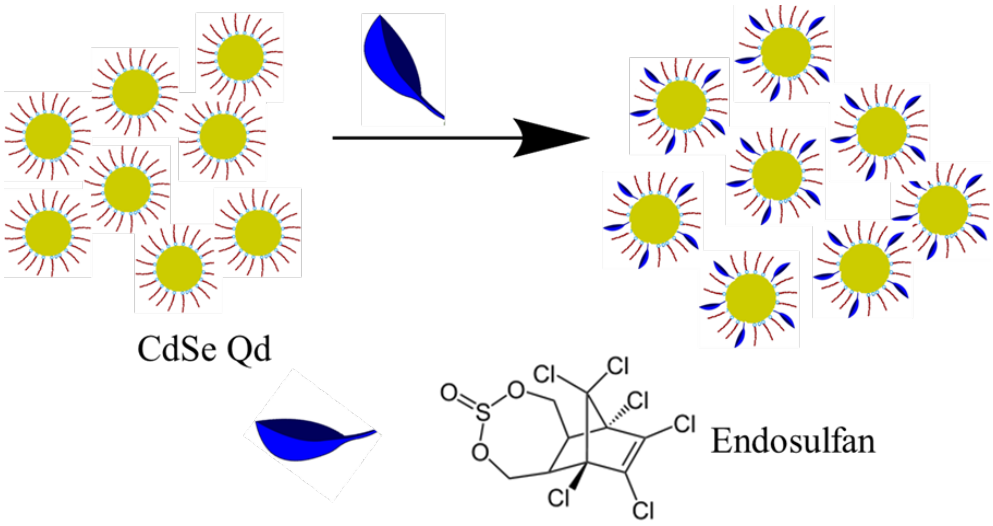

Scheme 1. Schematic representation of detection of endosulfan using CdSe Qd.

Again, XRD analysis confirmed the crystal structure of the Qd and Qd-ES systems. XRD (**Figure 4b**) of Qd shows cubic crystal structure with (111), (220), (311), and (222) planes at 2 theta values of 25.6°, 43.007°, 49°, and 52.66°. Upon the addition of ES, the crystal structure of Qd changed from cubic to hexagonal. It is due to the binding of the ES molecule through –S = O bonding (as reflected by the change in wavelength in the FTIR spectrum in **Figure A5** to the metal surface of Qd and the involvement of the hydrogen bond during the complexation. Due to the bulky nature of the ES molecule, the binding takes place diagonally, which leads to a change in crystal structure from cubic to hexagonal. After ES binding, the crystal planes of the system are (100), (002), (101), (102), (110), (103), and (201) at 2 theta values of 23.9°, 25.2°, 26.87°, 34.4°, 41.1°, 46.22°, and 52.0°, corresponding to a more stable hexagonal structure of CdSe quantum dots (**Figure 4b),** supporting the finding of the zeta potential study. All other un-assigned peaks in XRD correspond to planes of stabilizing agents for Qd and ES (**Figure 4b**). All the above observations are in favor of the attachment of endosulfan to the surface of Qd, enabling electronic transition and enhanced fluorescence with an increase in concentrations of ES.

The presence of endosulfan could be detected from the fluorescence enhancement, with the lowest limit of detection being 2 fM and the highest detection limit being 2 mM. Increasing the concentration of endosulfan beyond 2 mM showed saturation in the fluorescence signal without an appreciable increase.

The selectivity (**Figure 5**) of the quantum dot sensor towards other common analytes present in water was tested by adding 2 mM of the analytes to the sensor solution. There was no change in the fluorescence intensity with any of the commonly occurring analytes like cadmium (Cd), lead (Pb), copper (Cu), cobalt (Co), zinc (Zn), mercury (Hg), manganese (Mn), or magnesium (Mg). However, with the addition of endosulfan to the analyte-containing solution, an increase in fluorescence was observed, indicating the high selective detection of the pesticide in the presence of other analytes.

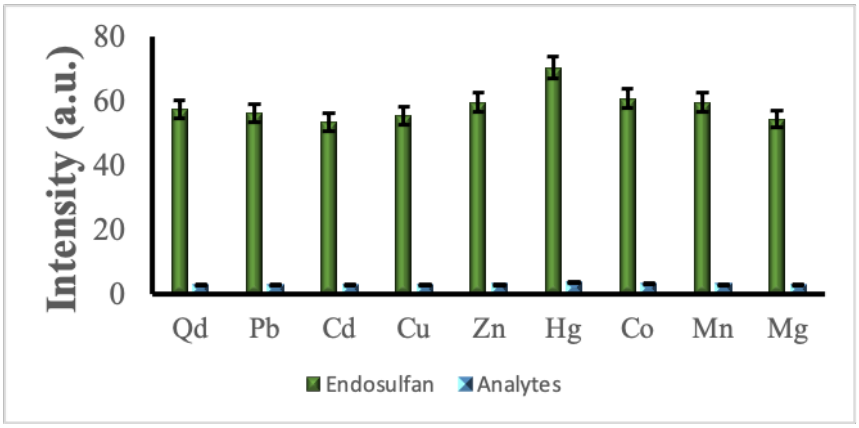

Figure 5. Selectivity of quantum dot sensor towards endosulfan upon addition of 2 mM concentration of different analytes and endosulfan (n = 3).

3.3. Detection of endosulfan in blood and milk

Detection of the presence of endosulfan in blood is equally or more important than detection in the environment because overexposure to the chemical can lead to its entry into the bloodstream through pesticide-contaminated food or water. So, we checked the efficacy of the Qd-based sensor in detecting endosulfan in blood (**Figures 6c** and **6d**). It also showed a concentration-dependent fluorescence enhancement similar to that of water.

Another route of entry for endosulfan is through cattle. If the cattle happen to feed on the endosulfan-treated fields, there is a chance of contamination of the cattle milk, which in turn can contaminate humans. So, the developed sensor was also checked for the detection of endosulfan from contaminated milk (**Figures 6a** and **6b**). In the case of milk, a slight broadening of the emission peak was observed with the addition of a Qd-based nanosensor. This can be due to the interaction of milk protein with Qd. But here also, the detection mechanism works perfectly, showing a concentration-dependent fluorescence enhancement with the addition of endosulfan-containing milk while retaining the broad emission pattern.

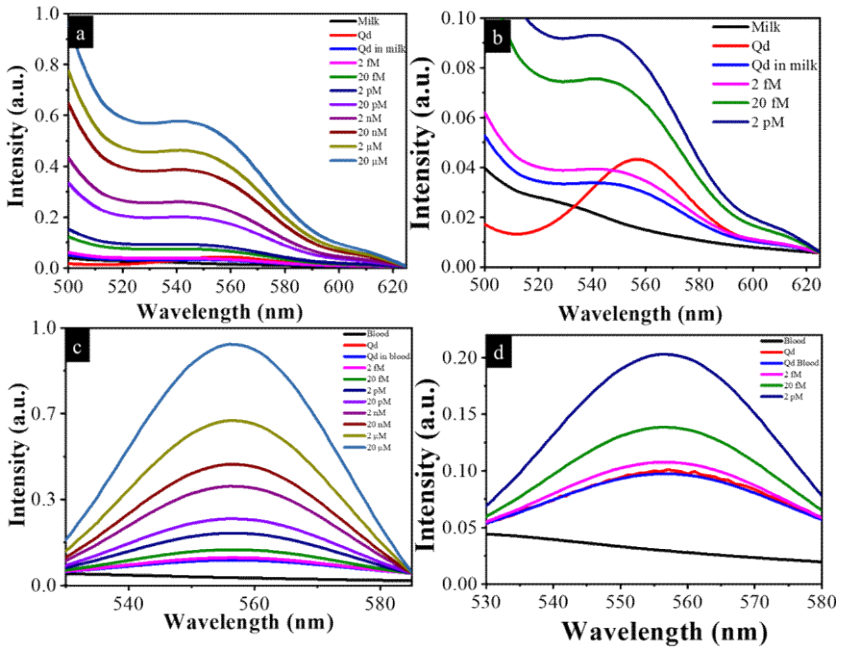

Figure 6. Endosulfan detection using the quantum dots in **(a)** milk and **(c)** blood. **(b)** and **(d)** are the fluorescence enhancement at lower ranges of endosulfan concentration re-plotted from **(a)** and **(c)**.

3.4. Comparison of the sensor in different environment

The efficacy of the developed sensor in different environments was checked in comparison with the fluorescence intensity of the quantum dot. The comparison is shown in **Figures A6a** and **A6b**. The presence of endosulfan in well water, pond water, and DI water shows an almost uniform fluorescence response upon the addition of a quantum dot sensor. However, in the case of pipe water, the fluorescence enhancement is slightly less, especially at higher concentrations. This may be either due to the slight aggregation of quantum dots or the hindrance of some other molecules present in pipe water. But below 20 nM, the response of endosulfan to quantum dots is almost uniform.

3.5. Removal of endosulfan from water

As the attachment of endosulfan to the quantum dots during its detection is strong and stable, as indicated by the enhanced fluorescence and changes in zeta potential and XRD analysis, endosulfan, along with Qd, can be removed from the contaminated system without its dissociation. Easy methods like centrifugation would suffice for this purpose. This was tested in water treated with different concentrations of endosulfan by centrifugation at 15,000 rpm for 15 min. Subsequently, the colourless supernatant and the pellet were independently treated with a freshly prepared quantum dot to test for the presence of endosulfan. The supernatant of water treated with endosulfan at concentrations up to 2 mM didn't show any considerable change in the fluorescence of the quantum dot, indicating that the developed system can remove the pesticide up to this concentration. When a higher concentration of 10 mM endosulfan was added, the supernatant showed a fluorescence enhancement corresponding to 20 fM (**Figure 7**).

4. Conclusion

In the present study, we have developed a highly selective sensor for the detection of endosulfan based on the changes in the emission of the sensor in the visible range. The sensing mechanism has been successfully demonstrated in different endosulfan-contaminated environments like pond water, well water, pipe water, blood, and milk. The sensor works successfully to detect the presence of this harmful pesticide at a limit as low as 2 fM. The higher limit was 2 mM. The presence of other heavy metal ions present in water has not affected the sensing, proving its high selectivity. It is also shown that the pesticide can be removed from the contaminated system at concentrations of the order of 2 mM. Validation of the current system with other existing methods is in progress.

Author contributions

Conceptualization, LVN and RSJ; methodology, LVN and RVN; validation, LVN, RVN and RSJ; formal analysis, LVN, RVN and RSJ; investigation, LVN, RVN and RSJ; resources, RSJ; writing—original draft preparation, LVN and RVN; writing—review and editing, RSJ; supervision, RSJ; project administration, RSJ; funding acquisition, RSJ.

Acknowledgments

RSJ acknowledges the Department of Biotechnology, Government of India for the financial support of the project BT/PR27222/NNT/28/1337/2017.

Conflict of interest

The authors declare that they have no conflict of interest.

References

1. Guerrini L, Aliaga AE, Cárcamo J, et al. Functionalization of Ag nanoparticles with the bis-acridinium lucigenin as a chemical assembler in the detection of persistent organic pollutants by surface-enhanced Raman scattering. *Analytica Chimica Acta* 2008; 624(2): 286–293. doi: 10.1016/j.aca.2008.06.038
2. Paul V, Balasubramaniam E, Kazi M. The neurobehavioural toxicity of endosulfan in rats: A serotonergic involvement in learning impairment. *European Journal of Pharmacology: Environmental Toxicology and Pharmacology* 1994; 270(1): 1–7. doi: 10.1016/0926-6917(94)90074-4
3. Sinha N, Adhikari N, K. Saxena D. Effect of endosulfan during fetal gonadal differentiation on spermatogenesis in rats. *Environmental Toxicology and Pharmacology* 2001; 10(1–2): 29–32. doi: 10.1016/s1382-6689(01)00066-7
4. Saiyed H, Dewan A, Bhatnagar V, et al. Effect of endosulfan on male reproductive development. *Environmental Health Perspectives* 2003; 111(16): 1958–1962. doi: 10.1289/ehp.6271
5. Wilkes PS. Gas-liquid chromatographic-mass spectrometric confirmation of endosulfan and endosulfan sulfate in apples and carrots. *Journal of AOAC International* 1981; 64(5): 1208–1210. doi: 10.1093/jaoac/64.5.1208
6. Ishaq Z, Nawaz MA. Analysis of contaminated milk with organochlorine pesticide residues using gas chromatography. *International Journal of Food Properties* 2018; 21(1): 879–891. doi: 10.1080/10942912.2018.1460607
7. Siddique T, Zahir ZA, Frankenberger WT. Reversed-phase liquid chromatographic method for analysis of endosulfan and its major metabolites. *Journal of Liquid Chromatography & Related Technologies* 2003; 26(7): 1069–1082. doi: 10.1081/jlc-120020094
8. Zhou X, Guan S, Li N, et al. Development of indirect competitive ELISA and colloidal gold immunochromatographic strip for endosulfan detection based on a monoclonal antibody. *Foods* 2023; 12(4): 736. doi: 10.3390/foods12040736
9. Shah M, Kolhe P, Gandhi S. Nano-assembly of multiwalled carbon nanotubes for sensitive voltammetric responses for the determination of residual levels of endosulfan. *Chemosphere* 2023; 321: 138148. doi: 10.1016/j.chemosphere.2023.138148
10. Division of Toxicology and Human Health Sciences. Public health statement for endosulfan. Available online: https://www.atsdr.cdc.gov/toxprofiles/tp41-c1-b.pdf (accessed on 8 January 2024).
11. Nsibande SA, Forbes PBC. Fluorescence detection of pesticides using quantum dot materials—A review. *Analytica Chimica Acta* 2016; 945: 9–22. doi: 10.1016/j.aca.2016.10.002
12. Priyadarshini E, Pradhan N. Gold nanoparticles as efficient sensors in colorimetric detection of toxic metal ions: A review. *Sensors and Actuators B: Chemical* 2017; 238: 888–902. doi: 10.1016/j.snb.2016.06.081
13. Saha K, Agasti SS, Kim C, et al. Gold nanoparticles in chemical and biological sensing. *Chemical Reviews* 2012; 112(5): 2739–2779. doi: 10.1021/cr2001178
14. Eustis S, El-Sayed MA. Why gold nanoparticles are more precious than pretty gold: Noble metal surface plasmon resonance and its enhancement of the radiative and nonradiative properties of nanocrystals of different shapes. *Chemical Society Reviews*. 2006; 35(3): 209–217. doi: 10.1039/b514191e
15. Nair RV, Nair LV, Govindachar DM, et al. Luminescent gold nanorods to enhance the near-infrared emission of a photosensitizer for targeted cancer imaging and dual therapy: Experimental and theoretical approach. *Chemistry—A European Journal* 2020; 26(13): 2826–2836. doi: 10.1002/chem.201904952
16. Nair RV, Radhakrishna Pillai Suma P, Jayasree RS. A dual signal on-off fluorescent nanosensor for the simultaneous detection of copper and creatinine. *Materials Science and Engineering: C* 2020; 109: 110569. doi: 10.1016/j.msec.2019.110569
17. Nair LV, Philips DS, Jayasree RS, et al. A near-infrared fluorescent nanosensor (AuC@Urease) for the selective detection of blood urea. *Small* 2013; 9(16): 2673–2677. doi: 10.1002/smll.201300213
18. Nair LakshmiV, Nagaoka Y, Maekawa T, et al. Quantum dot tailored to single wall carbon nanotubes: A multifunctional hybrid nanoconstruct for cellular imaging and targeted photothermal therapy. *Small* 2014; 10(14): 2771–2775. doi: 10.1002/smll.201400418
19. Suma PRP, Nair RV, Paul W, et al. Vanadium pentoxide nanoplates: Synthesis, characterization and unveiling the intrinsic anti-bacterial activity. *Materials Letters* 2020; 269: 127673. doi: 10.1016/j.matlet.2020.127673
20. Daniel MC, Astruc D. Gold nanoparticles: Assembly, supramolecular chemistry, quantum-size-related properties, and applications toward biology, catalysis, and nanotechnology. *Chemical Reviews* 2003; 104(1): 293–346. doi: 10.1021/cr030698+
21. Jibin K, Prasad JS, Saranya G, et al. Optically controlled hybrid metamaterial of plasmonic spiky gold inbuilt graphene sheets for bimodal imaging guided multimodal therapy. *Biomaterials Science* 2020; 8(12): 3381–3391. doi: 10.1039/d0bm00312c
22. Nair RV, Santhakumar H, Jayasree RS. Gold nanorods decorated with a cancer drug for multimodal imaging and therapy. *Faraday Discussions* 2018; 207: 423–435. doi: 10.1039/c7fd00185a
23. Santhakumar H, Nair ResmiV, Philips DS, et al. Real time imaging and dynamics of hippocampal Zn^{2+} under epileptic condition using a ratiometric fluorescent probe. *Scientific Reports* 2018; 8(1). doi: 10.1038/s41598-018-27029-5

24. Nair LV, Nair RV, Shenoy SJ, et al. Blood brain barrier permeable gold nanocluster for targeted brain imaging and therapy: An in vitro and in vivo study. *Journal of Materials Chemistry B* 2017; 5(42): 8314–8321. doi: 10.1039/c7tb02247f
25. Nair LV, Nazeer SS, Jayasree RS, et al. Fluorescence imaging assisted photodynamic therapy using photosensitizer-linked gold quantum clusters. *ACS Nano* 2015; 9(6): 5825–5832. doi: 10.1021/acsnano.5b00406
26. Chan WCW, Nie S. Quantum dot bioconjugates for ultrasensitive nonisotopic detection. *Science* 1998; 281(5385): 2016–2018. doi: 10.1126/science.281.5385.2016
27. Algar WR, Tavares AJ, Krull UJ. Beyond labels: A review of the application of quantum dots as integrated components of assays, bioprobes, and biosensors utilizing optical transduction. *Analytica Chimica Acta* 2010; 673(1): 1–25. doi: 10.1016/j.aca.2010.05.026
28. Li M, Chen T, Gooding JJ, et al. Review of carbon and graphene quantum dots for sensing. *ACS Sensors* 2019; 4(7): 1732–1748. doi: 10.1021/acssensors.9b00514
29. Deepak TS, Shenoy RS, Manonmani HK. Development of fluorescence immunoassay based on cadmium sulphide (cds) quantum dots for the detection of endosulfan. *International Journal of Current Advanced Research* 2016; 5(4): 744–748.
30. Sreekumaran Nair A, Tom RT, Pradeep T. Detection and extraction of endosulfan by metal nanoparticles. *Journal of Environmental Monitoring* 2003; 5(2): 363–365. doi: 10.1039/b300107e
31. Bakhsh H, Buledi JA, Khand NH, et al. NiO nanostructures based functional none-enzymatic electrochemical sensor for ultrasensitive determination of endosulfan in vegetables. *Journal of Food Measurement and Characterization* 2021; 15(3): 2695–2704. doi: 10.1007/s11694-021-00860-7
32. Goel P, Arora M. Fabrication of chemical sensor for organochlorine pesticide detection using colloidal gold nanoparticles. *MRS Communications* 2018; 8(3): 1000–1007. doi: 10.1557/mrc.2018.125
33. Masibi KK, Fayemi OE, Adekunle AS, et al. Electrochemical detection of endosulfan using an AONP-PANI-SWCNT modified glassy carbon electrode. *Materials* 2021; 14(4): 723. doi: 10.3390/ma14040723
34. Amiri GR, Fatahian S, Mahmoudi S. Preparation and optical properties assessment of CdSe quantum dots. *Materials Sciences and Applications* 2013; 04(02): 134–137. doi: 10.4236/msa.2013.42015
35. Wang Z, Xiao X, Zou T, et al. Citric acid capped CdS quantum dots for fluorescence detection of copper ions (II) in aqueous solution. *Nanomaterials* 2018; 9(1): 32. doi: 10.3390/nano9010032

Appendix

Supplementary materials that are excluded in the main body of the paper are included in the appendix. These includes additional supporting data, like excitation spectrum of CdSe quantum dots which shows a maximum excitation at 448 nm with a shoulder band at 482 nm (A1), the fluorescence variation of the CdSe quantum dot sensor in different water sources (A2), the linear dependency of endosulfan detection in pond water and pipe water represented as regression co-efficient value (A3) UV-Visible absorbance spectra of Qd and Qd with different concentrations of endosulfan (A4), FT IR spectra of the sensor, endosulfan and endosulfan treated sensor (A5), Comparison of CdSe quantum dot in different environments containing different concentrations of endosulfan (A6) and the removal of endosulfan as tested on the supernatant of DI water treated with 10 mM of endosulfan (A7) showing only insignificant enhancement in the fluorescence even at higher concentration.

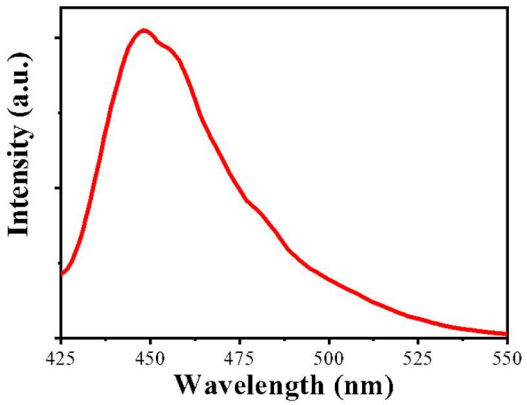

Figure A1. Excitation spectra of CdSe quantum dot.

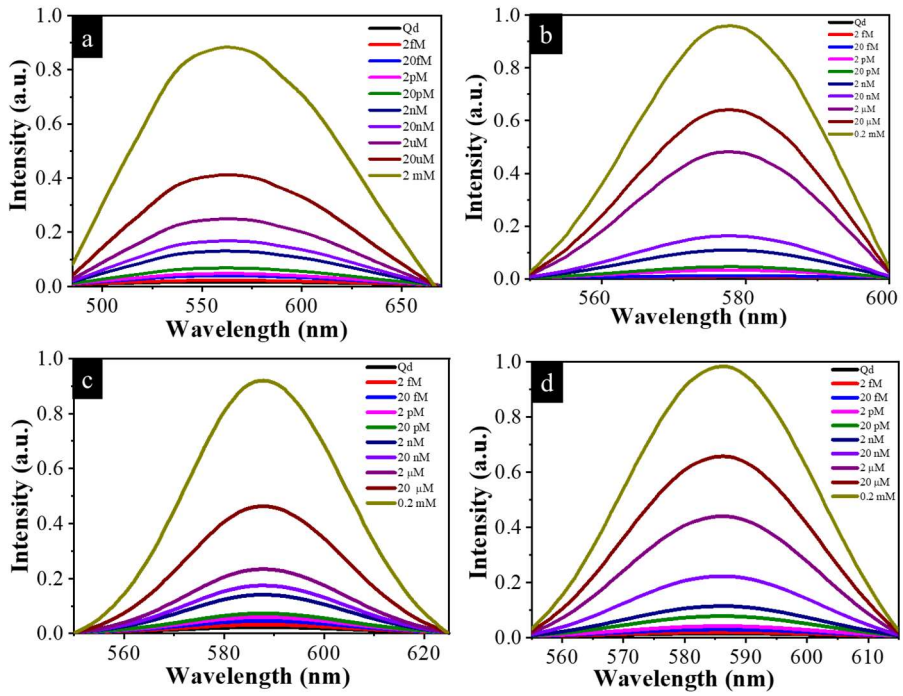

Figure A2. Endosulfan detection using the quantum dots in different water sources. Changes in the fluorescence of **(a)** DI water **(b)** well water, **(c)** pond water and **(d)** pipe water.

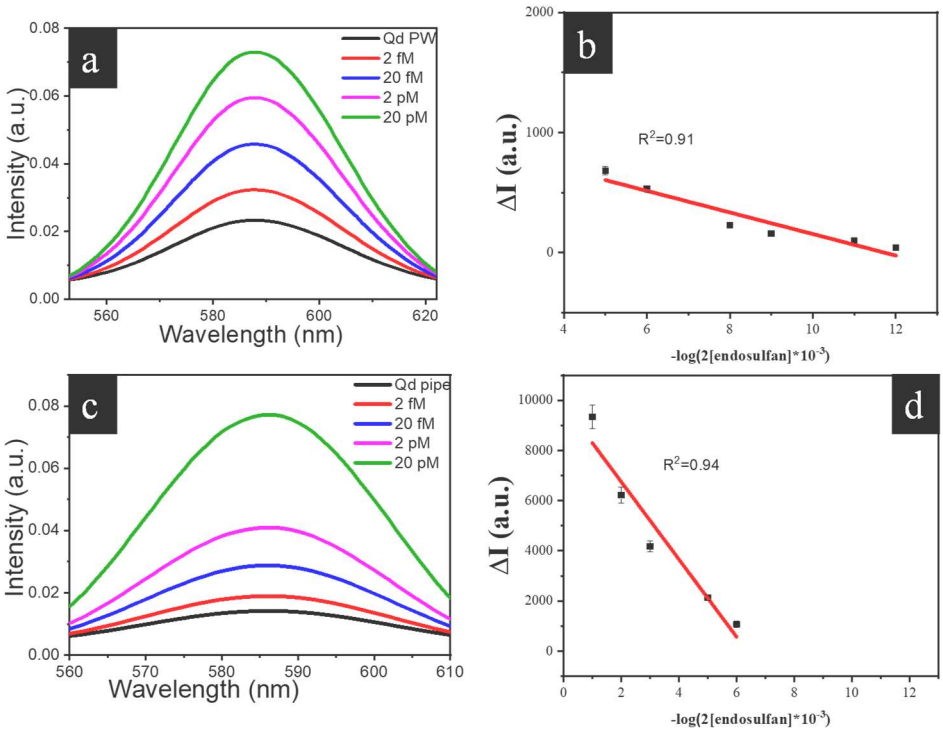

Figure A3. Endosulfan detection using the quantum dots in **(a)** Pond water, **(b)** corresponding linear relation from millimolar to femtomolar range, **(c)** pipe water and **(d)** corresponding linear relation from millimolar to femtomolar range.

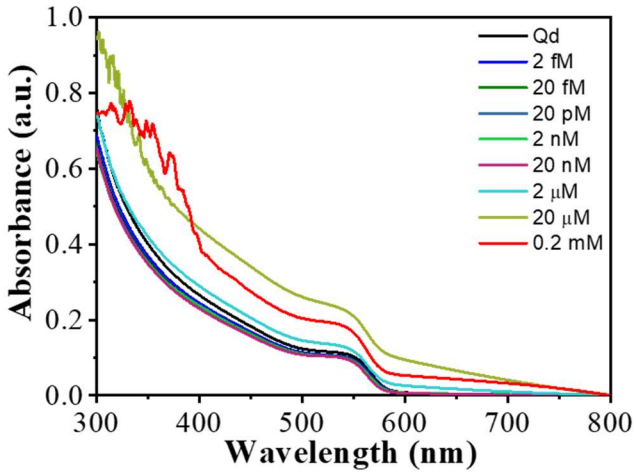

Figure A4. UV-visible absorbance spectra of Qd and Qd with different concentrations of endosulfan.

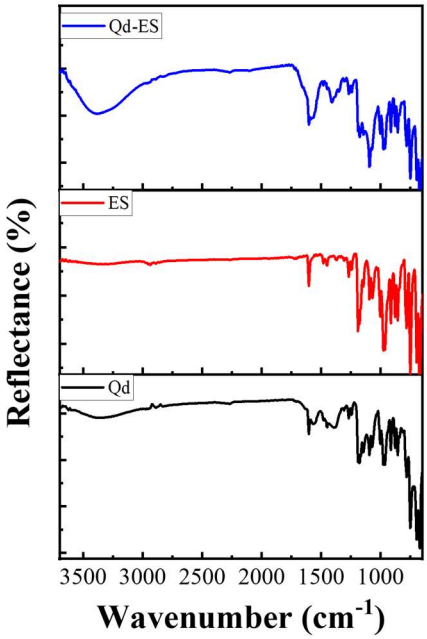

Figure A5. FT IR spectra of Qd, endosulfan and endosulfan treated Qd.

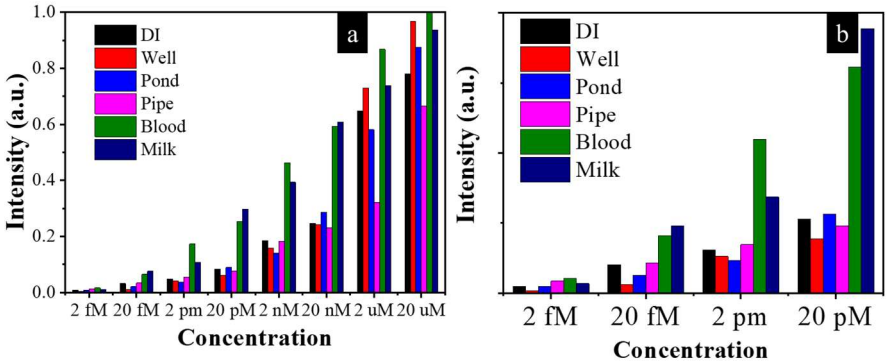

Figure A6. (a) Comparison of CdSe quantum dot in different environments containing different concentrations of endosulfan ranging from 2 fM to 20 µM, **(b)** shows the lower concentration (1 fM–20 pM) portions of **(a)**.

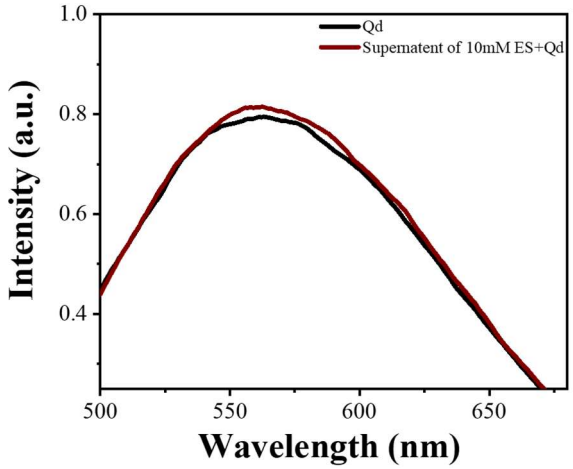

Figure A7. Fluorescence spectra of supernatant of Qd along with 10 mM endosulfan after adding freshly prepared Qd.